

Mechanical response of an inclined frictional granular layer approaching unjamming

A. P. F. ATMAN¹, P. CLAUDIN², G. COMBE³ and R. MARI²

¹ *Departamento de Física e Matemática and National Institute of Science and Technology for Complex Systems, Centro Federal de Educação Tecnológica de Minas Gerais, CEFET - MG - Av. Amazonas 7675, 30510-000, Belo Horizonte-MG, Brazil*

² *Laboratoire de Physique et Mécanique des Milieux Hétérogènes, (PMMH UMR 7636 CNRS - ESPCI - Univ. P. et M. Curie - Univ. Paris Diderot) - 10 rue Vauquelin, 75231 Paris Cedex 05, France, EU*

³ *UJF-Grenoble 1, Grenoble-INP, CNRS UMR 5521, 3SR Lab. - B.P. 53, 38041 Grenoble Cedex 09, France, EU*

received 2 November 2012; accepted in final form 4 February 2013

published online 1 March 2013

PACS 45.70.-n – Granular systems

PACS 46.25.-y – Static elasticity

PACS 64.60.av – Cracks, sandpiles, avalanches, and earthquakes

Abstract – We present an orthotropic elastic analysis of frictional granular layers under gravity by studying their stress response to a localized overload at the layer surface for several substrate tilt angles. The distance to the unjamming transition is controlled by the tilt angle α with respect to the critical angle α_c . We find that the shear modulus of the system decreases with α , but reaches a finite value as $\alpha \rightarrow \alpha_c$. We also analyze the vibration modes of the system and show that the soft modes play an increasing, though not crucial, role approaching the transition.

Copyright © EPLA, 2013

Various amorphous materials, and granular media in particular, exhibit a so-called jamming transition between rigid and flowing states. The nature of this transition has been investigated during the last decade, see recent reviews [1,2]. Most granular studies have focused on frictionless discs or spheres, typically controlled in volume fraction ϕ or in pressure P [3–5], showing that the jamming transition is critical (scaling exponents, diverging length scale) [3,6,7] and related to isostaticity [3,8–11]. As the system loses its mechanical rigidity at the transition, its shear modulus G is found to vanish as a power law with respect to the distance to jamming $\phi - \phi_c$, where ϕ_c is the critical volume fraction. Vibrational mode analyses have been performed on these frictionless granular systems [3,6,12–14], or similarly on soft glassy materials [15–17], reporting an increasing number of soft modes, corresponding to collective low-energy motion of the particles, as the transition is approached.

Much fewer studies have dealt with frictional grains in this context and they have mostly considered homogeneous systems under isotropic pressure [11,18–22]. In the frictional case, the Liu-Nagel jamming concept [23,24] must be revised [25]. In particular, jamming and isostatic points do not coincide any more [1], and one thus can expect a finite shear modulus at the transition.

In this letter, we consider static layers of frictional grains under gravity, by means of two-dimensional discrete element simulations (standard molecular dynamics [26]), and investigate their mechanical properties through the analysis of their stress response to a localized overload \vec{F}_0 at the layer surface. The layers are prepared at a fixed angle α with respect to the horizontal (see fig. 2 for notations), and unjamming is approached as α is close to α_c , the critical value above which static layers cannot be equilibrated at that angle and always flow. Note that this unjamming point α_c is close in spirit to the situation of a jammed solid sheared up to its yield-stress [27]. It is also close, but different, to progressively tilted granular layers, which eventually lose their mechanical stability, see, e.g., [28,29]. In our simulations, the volume fraction in the layer is fairly uniform all through the layer depth. Its value depends very weakly on the inclination angle, varying from $\phi \simeq 0.823$ at $\alpha = 0$ to $\phi \simeq 0.816$ at α_c (these are for the GG preparation, see below). These values are always larger —though not much— than the critical value, estimated in our system at $\phi_c \simeq 0.815$ [21,30,31]. Then, here, the control parameter for the jamming/unjamming transition is the sole angle α . This situation is therefore qualitatively different to the homogeneous configurations submitted to

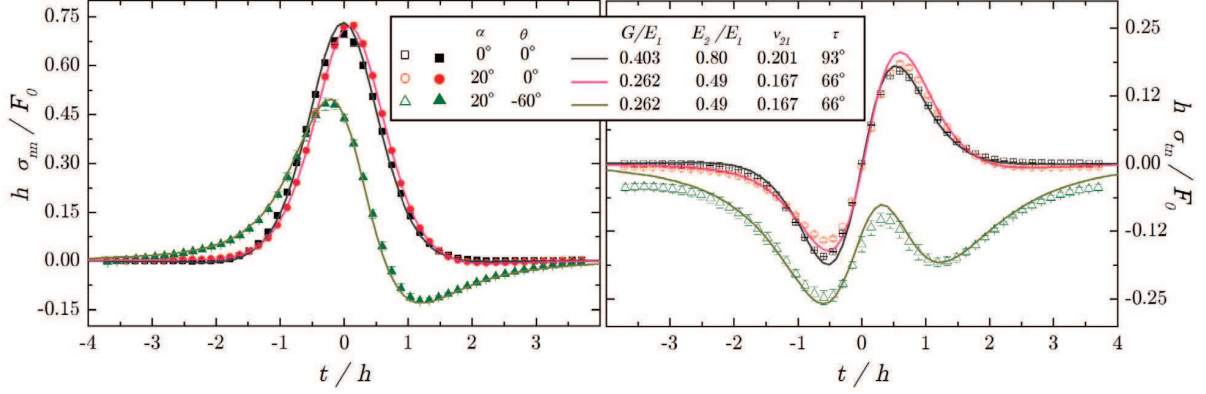


Fig. 1: (Colour on-line) Left panel: normal stress response profile σ_{nn} for two values of α , and two values of θ (see legend). Symbols: numerical data from the MD simulations (GG preparation, [32]). Solid lines: best elastic fit (see parameters in the legend). The stresses are normalized by F_0/h and the distance by h . Right panel: same for the shear stress response σ_{tn} .

isotropic pressure cited above, and is effectively closer to an experimental set-up.

The numerical model is that described in [32,33], with $N=3600$ polydisperse frictional discs coupled, when overlapping, by normal and tangential linear springs, tangential forces being limited by the Coulomb condition with a friction coefficient $\mu=0.5$. Two system preparations have been considered: a grain-by-grain (GG) and a rain-like (RL) deposition of the particles on a rough substrate consisting of fixed but size-distributed particles, inclined at the desired angle α . The layer is prepared when all grains have reached static equilibrium (see [32] for a description of these protocols). No external pressure applied to the topmost layer of particles, *i.e.*, the pressure in the system is due solely to the gravitational force acting on the particles themselves. The typical thickness of the layer is $\simeq 23$ grain diameters, *i.e.*, a system aspect ratio around 1/7. Above a certain inclination α_c , the simulations preparing the packing before the response procedure do not converge towards a static layer —the grains always flow. The “solid-liquid” transition is rather abrupt ($\Delta\alpha \simeq 0.5^\circ$), allowing for a well-defined value of this critical angle: $\alpha_c \simeq 20.75^\circ$ for the GG and $\alpha_c \simeq 20^\circ$ for the RL preparations, respectively. For the sake of concision, except otherwise stated, the displayed data are those obtained with the GG preparation.

Experimental and numerical works have shown that the linear stress response of granular systems to a point force is well described by (possibly anisotropic) elasticity [32, 34–38]. Here we show that an orthotropic elastic model is able to reproduce quantitatively the normal and tangential stress bottom profiles, and that the corresponding shear modulus G decreases with α , in parallel to a decrease of the coordination number and minor changes in the micro-structure (fabric). However, it does not vanish at the transition, but reaches a finite value as $\alpha \rightarrow \alpha_c$. We finally analyze the vibration modes of the system and show

that the soft modes play an increasing, though not crucial, role approaching the transition.

Stress response functions. — Once a layer is deposited, stabilized in an equilibrium state, an additional force \vec{F}_0 is applied on a grain close to the free surface, and a new equilibrium state is reached (see [32] for details). Taking the difference between the states after and before the overload, one can compute the contact forces in response to \vec{F}_0 . Introducing a coarse graining length w , the corresponding stress response can be determined. Taking w of the order of few mean grain diameters (here $w=6\langle d \rangle$) as well as an ensemble averaging of the data (here $N_e \sim 150$ realisations for each tilt angle α), make the stress profiles quantitatively comparable to a continuum theory [33], such as elasticity, as discussed below. The amplitude of the overload was kept constant for all simulations: $F_0 = 1.0 \langle m \rangle g$, where $\langle m \rangle$ is the average mass of the grains. This value is sufficiently small to ensure a linear [39,40] and reversible response of the system for all values of α , including close to α_c .

Three examples of stress bottom profiles $\sigma_{nn}(t)$ and $\sigma_{tn}(t)$ for the GG preparation are displayed in fig. 1 for two values of the slope α of the layer and two values of the angle θ that the overload force makes with the normal direction (see fig. 2). The stress profiles computed for the RL preparation have approximatively the same qualitative behavior.

Orthotropic elastic analysis. — In order to reproduce the stress response profile, isotropic elasticity is not enough [32], and we consider here orthotropic elasticity, characterized by a stiff axis (1) and a soft one (2) associated to two Young moduli E_1 and $E_2 < E_1$. Two Poisson coefficients ν_{12} and ν_{21} must also be introduced. However, they are not independent and verify $\nu_{12}/E_1 = \nu_{21}/E_2$. Finally, G is the shear modulus, so that the stress-strain

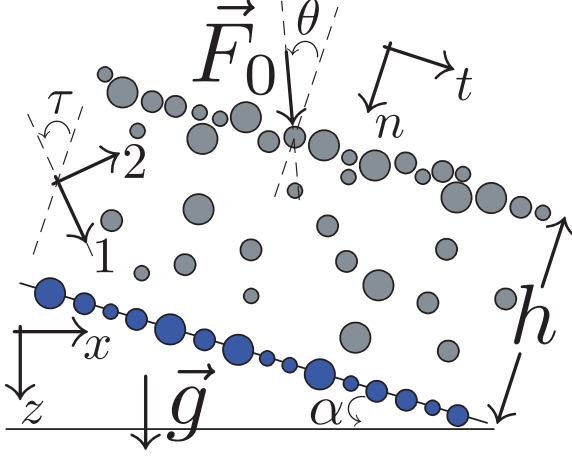


Fig. 2: (Colour on-line) Schematics of the system and notations. x is the horizontal axis. z is the vertical one, along which gravity \vec{g} acts. The granular layer, of average thickness h , is inclined at an angle α with respect to the horizontal axis. t and n are the axis, respectively, tangential and normal to the layer. A localized force \vec{F}_0 , which makes an angle θ with respect to n , is applied on a grain close to the surface of the layer. The stress responses σ_{nn} and σ_{tn} to this overload are measured at the bottom of the layer (fixed grains in blue). Axes (1, 2), making an angle τ with respect to (n, t) , are those of the orthotropic elastic analysis.

relation, in the orthotropic axis writes

$$\begin{pmatrix} \epsilon_{11} \\ \epsilon_{22} \\ \epsilon_{12} \end{pmatrix} = \begin{pmatrix} \frac{1}{E_1} & -\frac{\nu_{21}}{E_2} & 0 \\ -\frac{\nu_{12}}{E_1} & \frac{1}{E_2} & 0 \\ 0 & 0 & \frac{1}{2G} \end{pmatrix} \begin{pmatrix} \sigma_{11} \\ \sigma_{22} \\ \sigma_{12} \end{pmatrix}. \quad (1)$$

Elastic energy is well defined if all moduli E_1, E_2, G are positive and $1 - \nu_{12}\nu_{21} > 0$. A last parameter of this modeling is the angle τ that the axes (1, 2) make with (n, t) (see fig. 2).

The stress responses have been analytically computed in [41] for a semi-infinite layer ($h \rightarrow \infty$). For a finite layer thickness, a numerical integration, in the spirit of [34], must be done. Rough bottom boundary conditions (zero displacement) are imposed. We can adjust four dimensionless parameters (two modulus ratios G/E_1 and E_2/E_1 , a Poisson coefficient ν_{21} and the orthotropic angle τ) to reproduce, for a given α , the numerical data for all θ . As shown in fig. 1 (solid lines), the fitting functions quantitatively describe the numerical data.

In fig. 3, we show the behavior of the elastic modulus ratios G/E_1 and E_2/E_1 as the slope α is larger. They both decrease, almost by a factor of two, from a fairly constant value at small α to a lower one close to α_c . In particular, G does not vanish close to the critical angle, in agreement with the observation that frictional granular systems remain hyperstatic at the unjamming transition [11, 18, 19]. Such a discontinuous behaviour has been seen in simulations by Otsuki and Hayakawa [31]

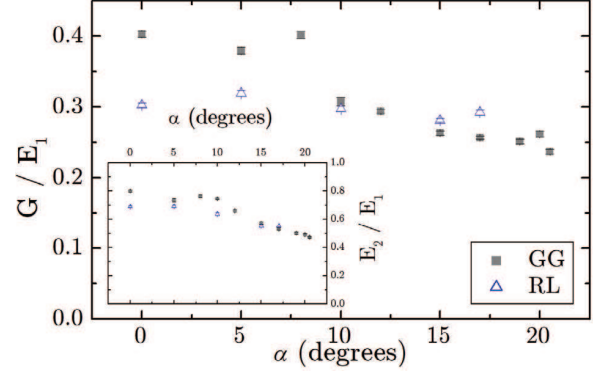


Fig. 3: (Colour on-line) Modulus ratio G/E_1 determined from the elastic fit, as a function of α , for two different layer preparations (see legend). Inset: same for E_2/E_1 .

investigating the rheology of sheared frictional grains close to jamming, and in experimentally created shear-jammed states reported in [25]. The ratio G/E_2 is almost constant (not shown). This behavior is also found for the RL preparation, although the variations of G/E_1 are less pronounced. This softening is finally consistent with acoustic experiments on a granular packing in the vicinity of the transition [42].

Microscopic variables. – In addition to the above global mechanical properties of the system, we have studied the evolution of various microscopic quantities with α . The first one of interest is the coordination number Z , *i.e.*, the average number of contacts per grain, here computed in the bulk of the layer, where it is fairly uniform —it obviously drops down close to the surface. Z monotonously decreases with α (fig. 4(a)) and stays always far from the isostatic value $Z_{\text{iso}} = 3$ (for frictional grains in 2D). As evidenced by the comparison of the curves in figs. 3 and 4(a), the modulus ratio G/E_1 is not found to be a linear function of $Z - Z_{\text{iso}}$, in contrast with the finding of [18] on homogeneous frictional systems, close to isostaticity. Grains of the bulk that only carry their own weight do not contribute much to the global stability of the contact network. As for so-called rattlers in gravity-free packings (see [43], Chapt. 6), these grains can be removed from the contact counting, leading to a modified coordination number of the layer Z^* (see fig. 4(a)). However, we have found that their number is roughly independent of α , so that the relation between G/E_1 and Z^* is not linear either. We have also studied the friction mobilisation at the contact level. In our MD simulations, the number of contacts with a ratio of the tangential force f_t to the normal force f_n strictly equal to the microscopic friction μ is zero when static equilibrium is reached. However, some of them are effectively close to the Coulomb criterion, and we have computed the average $\langle \frac{|f_t|}{\mu f_n} \rangle$. This quantity, displayed in fig. 4(a), increases

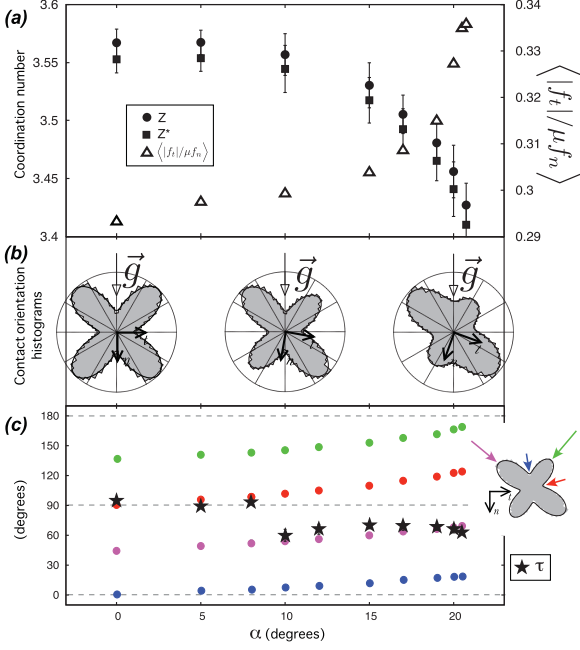


Fig. 4: (Colour on-line) (a) Evolution of the coordination number Z (●) with the inclination of the layer α . Taking into account “rattlers” (see text) gives a modified coordination number Z^* (■). Right y -axis: relative importance of friction mobilisation at contact (Δ). (b) Contact angle polar distributions (GG preparation) at $\alpha = 0, 10, 20^\circ$. Solid black line: fourth-order Fourier fit. Gravity is vertical (black arrow). (c) Fitted orthotropic elastic angle τ as a function of α (★). The four characteristic angles of the contact angle distribution, computed with respect to the direction n , are also shown—these angles correspond to the directions of the lobes, and to the directions in between the lobes, see sketch and corresponding coloured arrows.

as $\alpha \rightarrow \alpha_c$, but its overall variation is weak (see right y -scale).

Finally, we have studied the contact angle distribution. Three of these distributions are represented as polar diagrams for $\alpha = 0, 10$ and 20 degrees in fig. 4(b). The four strongly pronounced lobes are typical of the GG preparation [43] (Chapt. 6). The vertical and horizontal directions are always in between these lobes. When the layer is horizontal, the orthotropic stiff and soft directions are also found to be (almost) along the horizontal and vertical axis, respectively. Note that the fitting procedure effectively gives here $\tau = 93^\circ$ in this case, while $\tau = 90^\circ$ (or 0°) would have been expected for symmetry reasons. This indicates the typical precision we have on the measure of this orthotropic angle. Close to the critical slope, however, the orthotropic orientations are close to those of the lobes, the stiff one being in the direction of the slope. As evidenced in fig. 4(c), the transition between these two microscopic configurations occurs around $\alpha \simeq 9^\circ$, *i.e.*, well below α_c , in correspondence with the drop by a factor of 2 of G/E_1 between 8 and 10° (see fig. 3).

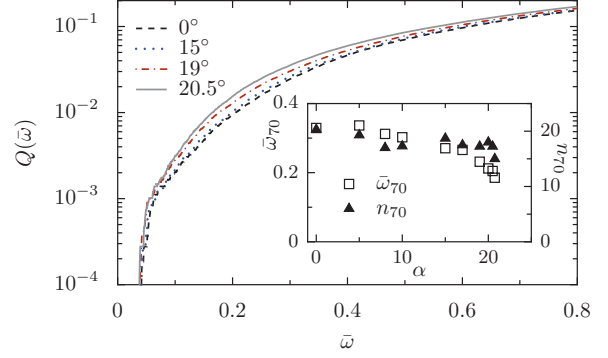


Fig. 5: (Colour on-line) Cumulative density of vibration modes $Q(\bar{\omega})$ for four different values of α (see legend). Inset: number of modes n_{70} , which are necessary to represent 70% of the displacement response, and the corresponding highest frequency $\bar{\omega}_{70}$, as a function of α .

Vibration mode analysis. — For each tilt angle α , we have computed the $3N$ vibration modes of the layer, performing a harmonic approximation of the energy around the equilibrium point reached by deposition of the grains. We only studied layers obtained by GG deposition. They do not show contacts being at the Coulomb threshold. This avoids the issue of the relevance of the harmonic approximation for such contacts [19]. Each contact between two grains is thus being considered as two linear springs (normal and tangential stiffnesses k_n and k_t ; here $k_t = 0.75k_n$). The reference vibration frequency is that of a single spring-mass system $\omega_0 = \sqrt{k_n / \langle m \rangle}$. We denote $D(\bar{\omega}) = (3N)^{-1} \sum_{\text{mode } i} \delta(\bar{\omega} - \bar{\omega}_i)$ and $Q(\bar{\omega}) = \int_0^{\bar{\omega}} D(\bar{\omega}') d\bar{\omega}'$, the density and cumulative density of states, where $\bar{\omega} = \omega / \omega_0$ is the normalized frequency.

The function Q is displayed in fig. 5 for four values of the slope α . No excess of vanishing frequencies are observed as the transition is approached, which is expected for a system that stays hyperstatic [44]. There is no single zero-frequency mode appearing at the transition either. The criticality of the layer thus cannot be described by the emergence of an energetically costless direction in configuration space. However, some rather soft modes ($0.1 \lesssim \bar{\omega} \lesssim 0.5$) are enhanced when $\alpha \rightarrow \alpha_c$. We have also computed the eigenfunctions corresponding to these modes. The displacement field in response to the overload with \vec{F}_0 can be decomposed on these functions, as they form a mathematical basis. We denote c_i the coefficients of this decomposition. A large part of the decomposition is owned by the 20 lowest frequency modes. Hence, we can compute the number of modes n_{70} which are necessary to represent 70% of the displacement field, and the highest frequency $\bar{\omega}_{70}$ of these n_{70} modes, by looking for the lowest frequency $\bar{\omega}_{70}$ such that $\sum_{i|\bar{\omega}_i < \bar{\omega}_{70}} c_i^2 > 0.70$. Both n_{70} and $\bar{\omega}_{70}$ are plotted against α in the inset of fig. 5. While n_{70} stays approximately constant and around 20, $\bar{\omega}_{70}$ is found to decrease from $\simeq 0.3$ by a factor of two when α varies from

zero to α_c , without however showing a clear singularity at the transition. This means that the response is progressively better represented by softer modes, even if these modes do not trigger the critical behavior of the layer close to the transition.

Conclusions. – To sum up, we have simulated 2D frictional and polydisperse granular layers under gravity inclined at an angle α , and investigated their mechanical and microscopic properties when the unjamming transition is approached. This work tells us what to expect in real experiments, *i.e.*, a layer that becomes elastically softer as $\alpha \rightarrow \alpha_c$, but not to the point at which the system would lose its rigidity before avalanching. Progressive enhancement of rather soft vibration modes should be observable, although they do not seem to play a particularly crucial role.

An interesting continuation of this work is to study this system with smaller and larger values of the contact friction coefficient μ . We have seen that GG layers prepared with $\mu = 0.1$ have a significantly smaller critical angle $\alpha_c \simeq 14^\circ$, whereas those prepared with $\mu = 10$ ($\alpha_c \simeq 21^\circ$) do not differ much from the case $\mu = 0.5$. Similarly, the grains are more connected and more densely packed at that critical angle in layers with $\mu = 0.1$ ($Z \simeq 3.6$ and $\phi \simeq 0.833$), whereas the values of Z and ϕ do not change much when the system is prepared with $\mu = 10$. However, the systematic investigation of the role of μ on the mechanical response of the granular layer, and on the elastic shear modulus in particular, is beyond the scope of the present paper. Another possible perspective could be to use granular simulations with a rolling resistance [45] in order to explore a wider range of ϕ , Z and α .

We thank B. ANDREOTTI, E. CLÉMENT, J. KURCHAN and M. TRULSSON for useful discussions and a careful reading of the manuscript. This work is part of the ANR JamVibe, project No. 0430 01. APFA has been partially supported by the exchange program “Science in Paris 2010” (Mairie de Paris). APFA thanks CNPq and FAPEMIG Brazilian agencies for financial funding.

REFERENCES

- [1] VAN HECKE M., *J. Phys.: Condens. Matter*, **22** (2010) 033101.
- [2] LIU A. J., NAGEL S. R., VAN SAARLOOS W. and WYART M., in *Dynamical Heterogeneities in Glasses, Colloids, and Granular Media*, edited by BERTHIER L., BIROLI G., BOUCHAUD J.-P., CIPELLETTI L. and VAN SAARLOOS W. (Oxford University Press, Oxford, UK) 2011, p. 298.
- [3] O’HERN C. S., LANGER S. A., LIU A. J. and NAGEL S. R., *Phys. Rev. Lett.*, **88** (2002) 075507.
- [4] O’HERN C. S., SILBERT L. E., LIU A. J. and NAGEL S. R., *Phys. Rev. E*, **68** (2003) 011306.
- [5] MAJMUDAR T. S., SPERL M., LUDING S. and BEHRINGER R. P., *Phys. Rev. Lett.*, **98** (2007) 058001.
- [6] WYART M., NAGEL S. R. and WITTEN T. A., *Europhys. Lett.*, **72** (2005) 486.
- [7] ELLENBROEK W. G., VAN HECKE M. and VAN SAARLOOS W., *Phys. Rev. E*, **80** (2009) 061307.
- [8] ROUX J.-N., *Phys. Rev. E*, **61** (2000) 6802.
- [9] MOUKARZEL C. F., *Granular Matter*, **3** (2001) 41.
- [10] TKACHENKO A. V. and WITTEN T. A., *Phys. Rev. E*, **60** (1999) 687.
- [11] AGNOLIN I. and ROUX J.-N., *Phys. Rev. E*, **76** (2007) 061302; 061303; 061304.
- [12] SILBERT L. E., LIU A. J. and NAGEL S. R., *Phys. Rev. Lett.*, **95** (2005) 098301.
- [13] DROCCO J. A., HASTINGS M. B., REICHHARDT C. J. O. and REICHHARDT C., *Phys. Rev. Lett.*, **95** (2005) 088001.
- [14] SCHRECK C. F., BERTRAND T., O’HERN C. S. and SHATTUCK M. D., *Phys. Rev. Lett.*, **107** (2011) 078301.
- [15] GHOSH A., CHIKKADI V. K., SCHALL P., KURCHAN J. and BONN D., *Phys. Rev. Lett.*, **104** (2010) 248305.
- [16] KAYA D., GREEN N. L., MALONEY C. E. and ISLAM M. F., *Science*, **329** (2010) 656.
- [17] CHEN K., ELLENBROEK W. G., ZHANG Z., CHEN D. T. N., YUNKER P. J., HENKES S., BRITO C., DAUCHOT O., VAN SAARLOOS W., LIU A. J. and YODH A. G., *Phys. Rev. Lett.*, **105** (2010) 025501.
- [18] SOMFAI E., VAN HECKE M., ELLENBROEK W. G., SHUNDYAK K. and VAN SAARLOOS W., *Phys. Rev. E*, **75** (2007) 020301.
- [19] HENKES S., VAN HECKE M. and VAN SAARLOOS W., *EPL*, **90** (2010) 14003.
- [20] HENKES S., SHUNDYAK K., VAN SAARLOOS W. and VAN HECKE M., *Soft Matter*, **6** (2010) 2935.
- [21] SILBERT L. E., *Soft Matter*, **6** (2010) 2918.
- [22] BRITO C., DAUCHOT O., BIROLI G. and BOUCHAUD J.-P., *Soft Matter*, **6** (2010) 3013.
- [23] LIU A. J. and NAGEL S. R., *Nature*, **396** (1998) 21.
- [24] LIU A. J. and NAGEL S. R., *Soft Matter*, **6** (2010) 2869.
- [25] BI D., ZHANG J., CHAKRABORTY B. and BEHRINGER R. P., *Nature*, **480** (2011) 355.
- [26] RAPAPORT D. C., *The Art of Molecular Dynamics Simulation* (Cambridge University Press, Cambridge, UK) 1995.
- [27] HEUSSINGER C. and BARRAT J.-L., *Phys. Rev. Lett.*, **102** (2009) 218303.
- [28] STARON L., VILOTTE J.-P. and RADJAÏ F., *Phys. Rev. Lett.*, **89** (2002) 204302.
- [29] HENKES S., BRITO C., DAUCHOT O. and VAN SAARLOOS W., *Soft Matter*, **6** (2010) 2939.
- [30] DA CRUZ F., EMAM S., PROCHNOW M., ROUX J.-N. and CHEVOIR F., *Phys. Rev. E*, **72** (2005) 021309.
- [31] OTSUKI M. and HAYAKAWA H., *Phys. Rev. E*, **83** (2011) 051301.
- [32] ATMAN A. P. F., BRUNET P., GENG J., REYDELLET G., COMBE G., CLAUDIN P., BEHRINGER R. P. and CLÉMENT E., *J. Phys.: Condens Matter*, **17** (2005) S2391.
- [33] GOLDENBERG C., ATMAN A. P. F., CLAUDIN P., COMBE G. and GOLDBIRSCH I., *Phys. Rev. Lett.*, **96** (2006) 168001.
- [34] SERERO D., REYDELLET G., CLAUDIN P., CLÉMENT E. and LEVINE D., *Eur. Phys. J. E*, **6** (2001) 169.

- [35] GOLDBIRSCH I. and GOLDENBERG C., *Eur. Phys. J. E*, **9** (2002) 245.
- [36] LEONFORTE F., TANGUY A., WITTMER J. P. and BARRAT J.-L., *Phys. Rev. B*, **70** (2004) 014203.
- [37] GOLDBIRSCH I. and GOLDENBERG C., *Nature*, **435** (2005) 188.
- [38] ATMAN A. P. F., BRUNET P., GENG J., REYDELLET G., CLAUDIN P., BEHRINGER R. P. and CLÉMENT E., *Eur. Phys. J. E*, **17** (2005) 93.
- [39] ATMAN A. P. F., CLAUDIN P., COMBE G., GOLDENBERG C. and GOLDBIRSCH I., in *Proceedings of the 6th International Conference on Micromechanics of Granular Media, Powders and Grains 2009*, edited by NAKAGAWA M. and LUDING S. (American Institute of Physics) 2009, p. 492.
- [40] ATMAN A. P. F., CLAUDIN P. and COMBE G., *Comput. Phys. Commun.*, **180** (2009) 612.
- [41] OTTO M., BOUCHAUD J.-P., CLAUDIN P. and SOCOLAR J. E. S., *Phys. Rev. E*, **67** (2003) 031302.
- [42] BONNEAU L., ANDREOTTI B. and CLÉMENT E., *Phys. Rev. Lett.*, **101** (2008) 118001.
- [43] RADJAÏ F. and DUBOIS F. (Editors), *Discrete-Element Modeling of Granular Materials* (ISTE, Wiley) 2011.
- [44] WYART M., SILBERT L. E., NAGEL S. R. and WITTEN T. A., *Phys. Rev. E*, **72** (2005) 051306.
- [45] ESTRADA N., TABOADA A. and RADJAÏ F., *Phys. Rev. E*, **78** (2008) 021301.